The Journal of Experimental Biology **199**, 1817–1828 (1996)
Printed in Great Britain © The Company of Biologists Limited 1996
JEB0408

MORPHOLOGY AND BIOMECHANICS OF THE MICROFIBRILLAR NETWORK OF SEA CUCUMBER DERMIS

FREDERICK A. THURMOND AND JOHN A. TROTTER
Department of Anatomy, University of New Mexico School of Medicine, Albuquerque, NM 87131, USA

Accepted 9 April 1996

Summary

The principal component of the body wall of the sea cucumber *Cucumaria frondosa* is a dermis consisting of collagen fibrils, microfibrils, proteoglycans and other soluble and insoluble components. A major structural constituent of the dermis is a network of 10–14 nm diameter microfibrils, which surrounds and penetrates bundles of collagen fibrils. This network has been extracted and purified using guanidine and bacterial collagenase. Tensile testing of the microfibrillar network in artificial sea water demonstrates that it is reversibly extensible up to approximately 300 % of its initial length. It behaves like a viscoelastic solid, having a long-range elastic component as well as a time-dependent viscous component. Reduction and alkylation of the cysteine residues in the network do not change its breaking strain or strength, but greatly increase the compliance of the network until, near the breaking strain, the tensile resistance rapidly increases. These data suggest that the strength of the network is due to non-reducible crosslinks, while its elasticity is dependent upon disulfide bonds. In deionized water, the network becomes swollen and, although it remains elastic, is much more compliant than when tested in artificial sea water. Examination of whole tissues and purified networks with the electron microscope reveals structures similar to vertebrate fibrillin-containing microfibrils. Considering that the dermis of *C. frondosa* is a mechanically mutable tissue in which elongation is accompanied by the sliding of collagen fibrils past one another, the microfibrillar network may act to maintain the orientation of fibrillar components during movement and may also provide a long-range restoring force.

Key words: microfibrils, echinoderm, fibrillin, elasticity, biomechanics, network, sea cucumber, *Cucumaria frondosa*.

Introduction

The dermis of the body wall of the sea cucumber *Cucumaria frondosa* (Echinodermata) is a connective tissue with mutable mechanical properties (Motokawa, 1984*a*,*b*; Trotter and Koob, 1995). These properties can be quickly and reversibly altered by the nervous system (Motokawa, 1984*b*; Wilkie, 1984; Motokawa, 1988). This ability to change the properties of the dermis is used in locomotion and protection, among other functions. The dermis is composed of collagen fibrils, proteoglycans, a microfibrillar network, other proteins and glycoproteins, nerve fibers and neurosecretory cells (Hyman, 1955; Motokawa, 1984*a*,*b*; Wilkie, 1984, 1996). Collagen fibrils, the most abundant structural element, are arranged into interwoven bundles. When the dermis is in the stiff state, caused by an interlinking of the fibrous elements, its material properties are similar to those of mammalian connective tissues (Motokawa, 1984*a*,*b*; F. A. Thurmond and J. A. Trotter, unpublished data). When it is in the compliant state, the collagen fibrils and bundles of fibrils can slide past one another. The dermis may change between stiff and compliant states in a matter of seconds. The collagen fibrils are similarly spindle-shaped and of high aspect ratio (Trotter *et al.* 1994). Because the fibrils lack any permanent interfibrillar crosslinks (Trotter *et al.* 1995) and must be able to slide past one another during lengthening and shortening of the tissue, there should be a structural component that surrounds and maintains the fibrils in bundles. Microfibrils have been reported as surrounding bundles of collagen fibrils in the crinoid arm stalk (Echinodermata) (Birenheide and Motokawa, 1994).

The dermis of *C. frondosa* possesses an extensive network of microfibrils. Previous work has suggested that the microfibrillar networks in echinoderms might consist of fibrillin microfibrils (Smith *et al.* 1981; Trotter and Koob, 1989; Candia Carnevali *et al.* 1990; Thurmond and Trotter, 1992; Wilkie *et al.* 1992*a*,*b*; Birenheide and Motokawa, 1994; Trotter *et al.* 1994). Biochemical and immunochemical characterization of the *C. frondosa* microfibrillar network has shown that it is composed primarily of a protein that strongly resembles mammalian fibrillin (F. A. Thurmond, T. J. Koob, J. M. Bowness and J. A. Trotter, in preparation). Because the microfibrils are found throughout the dermis, they have been postulated to be the structural elements that maintain the organization of the dermis during movements (Trotter and Koob, 1989; Wilkie, 1996). This

report describes the purification, morphology and material properties of this microfibrillar network. The results suggest that the fibrillin-like microfibrillar network in *C. frondosa* dermis is a continuously crosslinked elastomeric solid that confers long-range elasticity to this mutable tissue.

Materials and methods

Animals and tissue

Sea cucumbers, *Cucumaria frondosa* (Hyman, 1955), were collected from the Gulf of Maine (USA) and maintained for up to 2 months at the Mount Desert Island Biological Laboratory in a constantly flowing fresh seawater system, at a temperature of 12–15 °C. The studies described below were all performed on pieces of white inner dermis from the two ventral interambulacral regions, lacking podia (Hyman, 1955). The attached inner muscular layer was pulled off using tweezers, the pigmented outer dermis was removed using a razor blade, and the inner dermis was cut into specimens approximately 2.0 cm×0.5 cm×0.5 cm and stored at −70 °C.

Purification of microfibrillar networks

Tissue pieces were cut into uniform specimens 2.0 cm×0.2 cm×0.2 cm using razor blades and a fabricated cutting die. The specimens were extracted in a solution of 6 mol l^{-1} guanidine–HCl, 50 mmol l^{-1} sodium acetate, pH 6.0, 10 mmol l^{-1} *N*-ethylmaleimide (NEM), at 4 °C for 24 h. All guanidine extractions were carried out in a volume of extraction buffer equal to 10 times the wet mass of the tissue: specimens were gently agitated during extraction (Nutator, Adams). The specimens were then extracted for another 24 h in fresh extracting solution under the same conditions, except that the concentration of NEM was 2 mmol l^{-1}. NEM was used to prevent artifactual disulfide bond formation. After the second guanidine extraction, the tissue was resuspended in the same volume of collagenase buffer, consisting of 200 mmol l^{-1} NaCl, 50 mmol l^{-1} Tris–HCl, 10 mmol l^{-1} $CaCl_2$, 3.1 mmol l^{-1} NaN_3, pH 7.4. Six changes of collagenase buffer were used to ensure complete removal of guanidine from the specimens. Protease inhibitors were added to the last change of collagenase buffer to give 1 mmol l^{-1} phenylmethylsulfonyl fluoride and 1 mmol l^{-1} NEM. Purified, crystallized collagenase (Sigma Chemical Co.; Type III, fraction A) was added to the solution at a concentration of 150 units of collagenase activity per gram of starting material (1 unit hydrolyses 1 μmol FALGPA per min at 25 °C in the presence of calcium ions). The tissue was exposed to collagenase for 24 h at 37 °C. If digestion was incomplete, as determined by visual inspection, more collagenase (approximately 100 units per gram of starting material) was added and incubation was continued for another 24 h. This method removed all of the collagen that could be detected by hydroxyproline assay of the hydrolyzed residue (20 p.p.m. detection limit) (Bergman and Loxly, 1963). The tissue specimens were then extracted for 24 h at 4 °C in four changes of 6 mol l^{-1} guanidine extraction buffer (described above) containing 1 mmol l^{-1} NEM. SDS–PAGE analysis of guanidine extracts showed that after the four final guanidine extractions there was no detectable extraction of proteins (data not shown).

Swelling and pH experiments

Specimens prepared as described above (termed GCG specimens) were placed either into water or into artificial sea water (ASW) containing 25 mmol l^{-1} Mops, 450 mmol l^{-1} NaCl, 50 mmol l^{-1} $MgCl_2$, 10 mmol l^{-1} KCl, 10 mmol l^{-1} $CaCl_2$, 3.1 mmol l^{-1} NaN_3, pH 8.0, and allowed to come to equilibration with gentle rocking. Each specimen was incubated for 8 h at 4 °C in a volume at least 2000 times the wet mass of the starting material.

To determine the volume change of specimens in unbuffered water at varying pH values, specimens were placed into solutions of specified pH (adjusted with concentrated HCl or NaOH). The pH of the solutions was monitored during the experiments. The tissues were incubated in a 2000-fold excess of water at a specific pH for at least 2 h before their dimensions were measured. The dimensions of specimens were measured immersed in fluid using a digital filar micrometer mounted to the eyepiece of an Olympus stereozoom dissecting microscope.

GCG and GCGRA (GCG specimens plus reduction and alkylation, see below) microfibrillar networks were equilibrated in water, blotted dry and weighed. They were then dried in an oven at 70 °C and weighed again. These values were used for calculating percentages of solid material and fluid in the specimens.

Reduction and alkylation

Specimens were reduced and alkylated using a modification of the method described by Means and Feeney (1975). After the fourth post-collagenase guanidine extraction, the specimens were incubated in 6 mol l^{-1} guanidine, 50 mmol l^{-1} sodium acetate, 3.1 mmol l^{-1} NaN_3, 50 mmol l^{-1} dithiothreitol (DTT) for 24 h at 4 °C. These specimens are termed GCGR specimens. If alkylation was to follow, the solution was replaced with one of the same composition containing 100 mmol l^{-1} iodoacetamide, and incubation was continued at 37 °C for 4 h in the dark. The specimens were then resuspended in ASW. These specimens are termed GCGRA specimens.

Transmission electron microscopy

Samples were removed during certain of the processing steps described above and prepared for electron microscopy. Tissues removed from guanidine extraction buffer were washed with ASW at least six times, for 2 h each, at a ratio of 100 ml ASW per 5 g of starting material. After equilibration in ASW, the tissue was prepared for transmission electron microscopy (TEM) by fixation in 2.5 % glutaraldehyde, 100 mmol l^{-1} Mops, 300 mmol l^{-1} NaCl, 50 mmol l^{-1} $MgCl_2$, 10 mmol l^{-1} KCl, 5 mmol l^{-1} $CaCl_2$, pH 8.0. After fixation for at least 24 h in the primary fixative, the specimens were rinsed with the same vehicle, lacking glutaraldehyde, for 12–24 h with several changes of solution. They were then immersed in 1 % osmium tetroxide in 0.1 mol l^{-1} sodium cacodylate buffer, for

1–2 h, rinsed in water, stained for 1–2 h with 0.5 % uranyl acetate in water, dehydrated in increasing concentrations of ethanol, and embedded in Spurr's resin. Thin sections were cut using a diamond knife, collected on 75×300 mesh oblong copper grids, and stained with uranyl acetate and lead citrate. TEM was carried out using a Hitachi H-600 electron microscope operated at 75 kV. Stereo pairs were made on the same electron microscope utilizing a tilting specimen holder.

One TEM preparation was made by stretching a GCG specimen that had been equilibrated in ASW. This specimen was originally 2.0 cm×0.2 cm×0.2 cm, and was affixed to a small C-shaped glass pipette using cyanoacrylate adhesive. The specimen was fixed with glutaraldehyde and osmium tetroxide at 250 % of its initial length, after which it was processed for electron microscopy as described above. The tissue was cut away from the glass pipette just before it was embedded in Spurr's resin. It did not noticeably shrink during the dehydration process and did not retract when it was detached from the glass pipette using a razor blade.

Some solutions were viewed using TEM by applying the sample to, and staining directly on, an electron microscope grid. The method consisted of applying 2 µl of the solution of interest to a formvar-coated electron microscope grid. After 1 min, the solution was drawn off using the edge of a filter paper and replaced with water. After two water washings, 1 % uranyl acetate in water was applied to the grid. After 1 min, the uranyl acetate was drawn off the grid and the grid was briefly (5 s) washed with water. The grid was then air-dried and examined using TEM.

Rotary shadowing

Samples were deposited onto freshly cleaved mica using a modification of the glycerol/volatile buffer method (Engel and Furthmayr, 1987). The specimen was mixed 1:1 with 0.4 mol l^{-1} NH_4HCO_3, pH 7.5, 80 % glycerol, giving final concentrations of 0.2 mol l^{-1} NH_4HCO_3 and 40 % glycerol. The solution was then quickly sprayed onto freshly cleaved mica with an atomizer. Specimens on mica were mounted on a rotating stage in a Balzers apparatus. The chamber was evacuated to below 1.33×10^{-6} Pa. The specimens were rotary-shadowed with platinum at an angle of 5 ° and subsequently coated with carbon at an angle of 90 °. The replicas were floated onto water and picked up on 400 mesh copper grids. They were viewed and micrographed using TEM.

Mechanical testing

A light-duty material testing device was fabricated from acrylic. This device is pictured in Fig. 1. The specimens were approximately 2 cm×2.0 mm×2.0 mm when clamped into this device. The device allowed loading of the beam at one end. The other end of the beam was attached to the specimen using surgical silk. Displacement of the beam, and therefore of the specimen, was measured by a linear variable displacement transducer (Lucas Schaevitz) connected to a chart recorder. One end of the specimen was glued using cyanoacrylate adhesive between two halves of an acrylic screw clamp and affixed to the bottom of an incubation vessel. The other end of the specimen was clamped in a similar acrylic clamp and attached to the end of the beam using surgical silk. A die that held the two clamps a fixed distance apart was used to ensure that the starting length of each specimen when initially clamped was 1 cm. The entire specimen remained completely submerged in buffer, with only the surgical silk exposed to air.

A constant temperature was maintained in the incubation vessel by coiled, coated copper tubing connected to a circulating cooling pump. The cooling pump was adjusted so that the temperature of the testing buffer was maintained at 12 °C.

After the specimen had been clamped in the apparatus, it was equilibrated (for at least 15 min with no load) in the testing buffer. It was then loaded with a known mass and, after 30 s, a second identical mass was added, and so on, for a total of

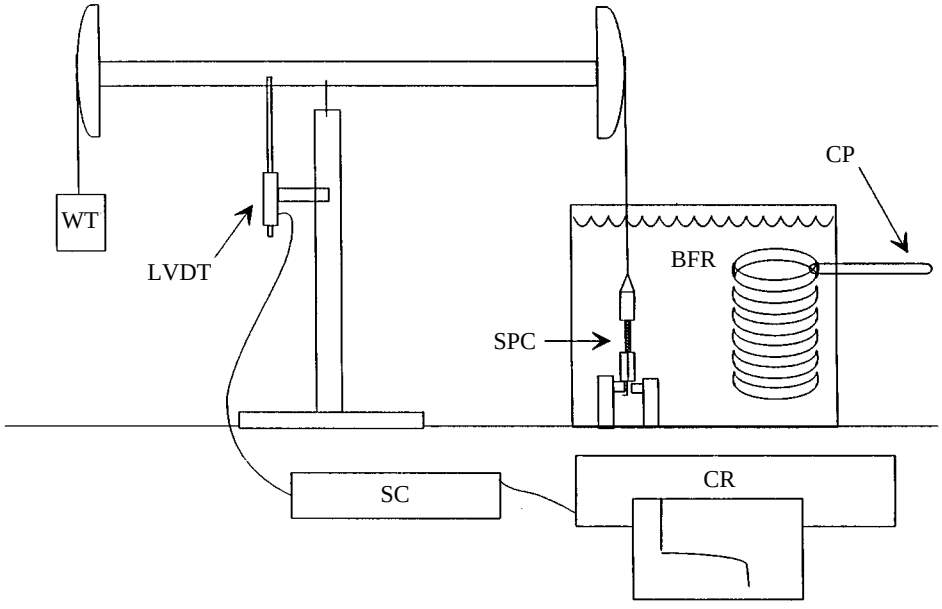

Fig. 1. Diagram of the mechanical testing apparatus. SPC, specimen; WT, weight; LVDT, linear variable displacement transducer; BFR, buffer; SC, signal conditioner; CR, chart recorder; CP, to cooling pump.

7–11 masses. The tissue was then allowed to recover for 30 min to its initial length. Its breaking strength was then measured by loading at 5 s intervals with relatively heavy masses (500 mg) until the specimen broke. From the data, it was possible to estimate elastic moduli and breaking strengths. The strain values used in this work represent 'conventional' or 'engineering' strain.

Results

Swelling behavior

Specimens that had been extracted in guanidine–HCl, digested with collagenase, re-extracted in guanidine–HCl (GCG, as described in Materials and methods) and equilibrated in ASW had approximately half the volume of untreated specimens (Table 1). Those that had been reduced and alkylated, in addition to the above (GCGRA), were slightly smaller still. The volumes of GCG specimens decreased further in water at pH 2, increased approximately threefold in water at pH 7 and increased approximately six- to sevenfold in water at pH 12. The volumes of GCGRA specimens increased almost 10-fold in water.

When GCG specimens in water were equilibrated sequentially in unbuffered solutions of decreasing pH, the volume decreased progressively (Table 2). The largest change occurred between pH 4 and pH 3, where volumes decreased from 0.87 to 0.31 times the initial volume.

Addition of any of the following salts to the water-swollen GCG specimens caused them to shrink markedly: ASW; 0.1–2.0 mol l^{-1} NaCl; 20 mmol l^{-1} $CaCl_2$; 20 mmol l^{-1} Mops; 20 mmol l^{-1} Tris–HCl; or 3.1 mmol l^{-1} NaN_3. GCG specimens could be sequentially equilibrated in water and ASW more than 10 times without disaggregating. Reduced and alkylated (GCGRA) specimens that had been swollen in water and subsequently equilibrated in ASW did not shrink homogeneously. Rather, they became somewhat irregular in shape and were quite fragile.

Table 1. *Effects of equilibration solutions on relative volumes of GCG and GCGRA microfibrillar network preparations*

Specimen	Volume relative to untreated volume in ASW
Untreated tissue in ASW	1.00
GCG in ASW	0.543±0.078*
GCGRA in ASW	0.417±0.025*
GCG in H_2O, pH 7.0	2.877±1.03
GCGRA in H_2O, pH 7.0	9.833±2.37*
GCG in H_2O, pH 2.0	0.310±0.009*
GCG in H_2O, pH 12.0	6.655±1.008*

GCG specimens were sequentially guanidine-extracted, collagenase-digested and guanidine-extracted.

GCGRA specimens were treated as GCG followed by reduction with dithiothreitol and alkylation with iodoacetamide.

ASW, artificial sea water.

Values are means ± S.D. (N=9).

*Values significantly different from 1.00 (P<0.05).

Table 2. *Effects of sequential application of unbuffered solutions of decreasing pH on relative volume and length of GCG microfibrillar network preparations*

pH of solution	Relative volume of specimen (GCG in ASW=1.0)	Relative length of specimen on long axis of body wall
7.0	1.00	1.00
4.0	0.87±0.02	0.95±0.03
3.0	0.31±0.10	0.66±0.08
2.5	0.17±0.02	0.55±0.04
2.0	0.16±0.01	0.53±0.03
1.5	0.14±0.01	0.51±0.01

GCG specimens were sequentially guanidine-extracted, collagenase-digested and guanidine-extracted.

ASW, artificial sea water.

N=6. Values are means ± S.D.

The mean mass ± S.D. of hydrated GCG specimens equilibrated with water was 216.33±11.4 mg (N=9), and after drying the mean mass was 1.49±0.09 mg. GCG specimens were therefore 99.31 % water and 0.69 % solid material. The volume of GCG specimens in water was 5.29 times their volume in ASW (Table 1). Thus, GCG specimens in ASW were estimated to be 3.65 % solid material and 96.35 % fluid. These values were used for the calculations below involving elastic modulus.

Transmission electron microscopy

Tissue sections

In untreated specimens, the spaces between bundles of collagen fibrils are occupied principally by microfibrils, which are also found between individual collagen fibrils (Fig. 2). An interweaving of the microfibrils in the bundles is suggested at higher magnification, along with a beaded structure (Fig. 2B).

GCG specimens retained the bundles of microfibrils (Fig. 3). The apparently empty spaces in the micrographs indicate the locations of collagen fibrils, which have been degraded and extracted. Some small cellular remnants can be seen. The morphology of the microfibrils does not appear to be changed by GCG treatment (compare Figs 2B and 3B). Cross-sectioned microfibrils appear to have a central region that is slightly less electron-dense, surrounded by a darkly staining pentagonal or hexagonal structure (Fig. 3B, inset).

Reduction of disulfide bonds (GCGR treatment) gives the microfibrils a stellate appearance (Fig. 4) characterized by an irregular perimeter. In addition, they appear clumped and less fibrillar (compare Figs 4B and 3B). Alkylation of sulfhydryl groups following reduction of disulfide bonds further changes the morphology of the network, mainly by increasing the distance between individual microfibrils (Fig. 5).

Negative staining

Guanidine-extracted and collagenase-treated microfibrillar specimens (GCG) were equilibrated in deionized water and

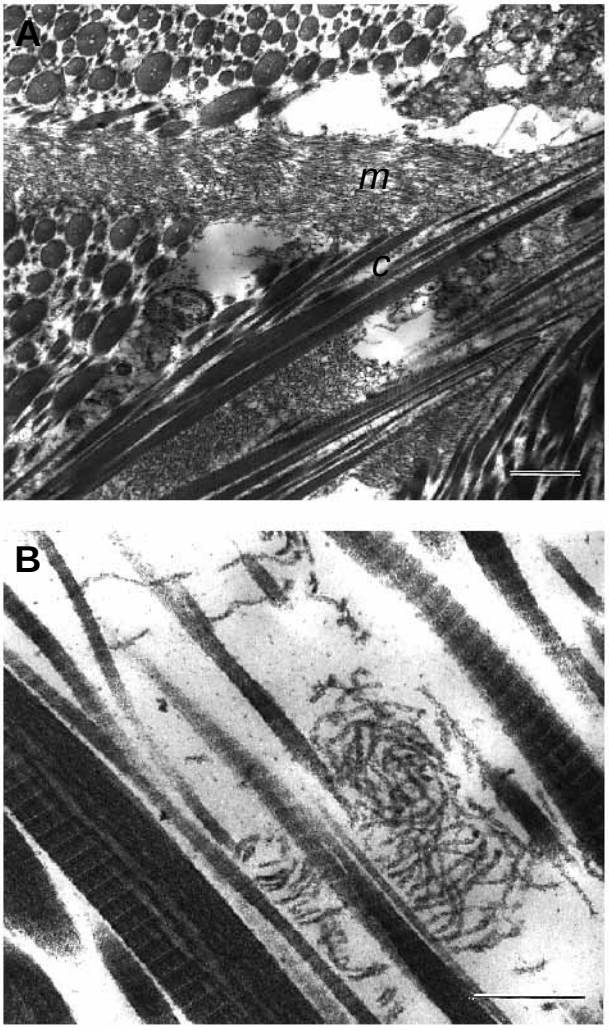

Fig. 2. Transmission electron micrographs of freshly frozen *Cucumaria frondosa* dermis. Bundles of collagen fibrils (*c*) and intervening columns of microfibrils (*m*) are visible. Scale bars, A, 1 μm; B, 300 nm.

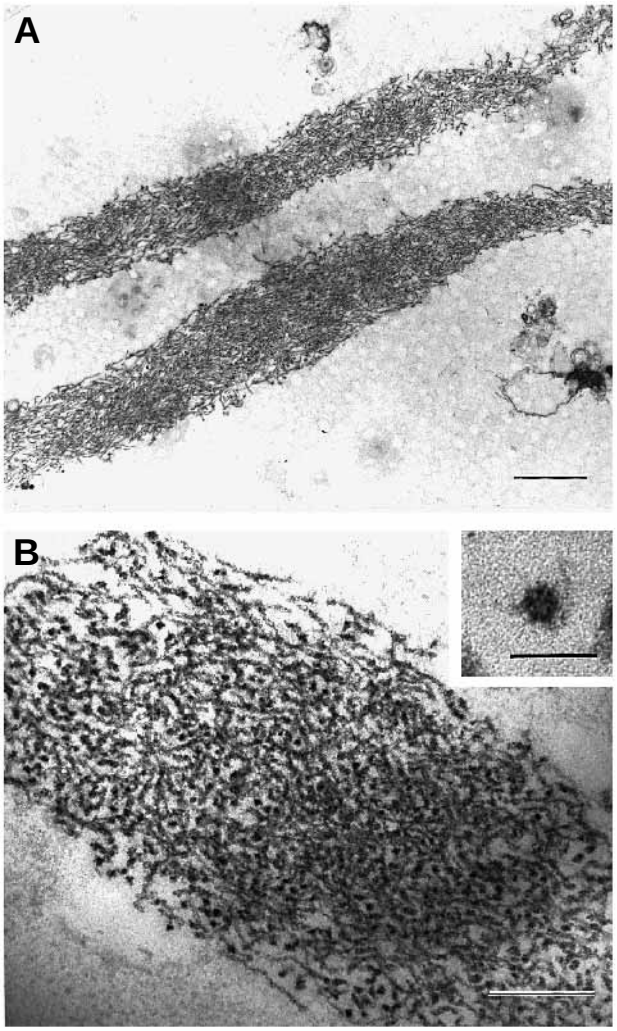

Fig. 3. Transmission electron micrographs of a GCG (see Materials and methods) microfibrillar preparation. The microfibrils do not appear altered compared with the control (Fig. 2). Inset, high-magnification of a cross section of a microfibril. Note the pentagonal shape and electron-lucent center. Scale bars, A, 1 μm; B, 300 nm, inset, 20 nm.

then subsequently homogenized using a Dounce homogenizer with a loose-fitting pestle. Negative staining of the preparation with uranyl acetate revealed microfibrils 23 nm in width (Fig. 6A) compared with the average diameter of 12 nm (range 10–14 nm) in fixed and plastic-embedded material.

After incubation in 20 mmol l^{-1} $CaCl_2$, 10 mmol l^{-1} Mops, pH 8.0, for 24 h, many microfibrils had smaller diameters (approximately 13 nm), appeared beaded in many regions and had an average interbead distance of 45 nm (arrowheads, Fig. 6B). Other microfibrils in the preparation appeared less beaded and were wider. Negatively stained reduced and alkylated microfibrils (Fig. 6C) lacked a filamentous substructure and appeared to have regularly occurring nodules on their surfaces which were frequently associated with kinks in the microfibrils.

Rotary shadowing

Rotary shadowing of GCG preparations following homogenization in ASW showed fine filaments extending outward from the regularly spaced beads (Fig. 7A). In a few specimens, the beads were not constantly spaced, showing a variable periodicity, from 30 to 100 nm (data not shown). In ASW, the filaments appeared to overlap one another. When the GCG preparation was equilibrated in deionized water and then Dounce-homogenized and rotary-shadowed, the filaments extending away from the beads did not appear to overlap one another to the degree that was seen in ASW (Fig. 7B,C). Some filaments projected as far as 80 nm away from their attachment to the bead (Fig. 7B, filled arrowhead), but most projected about 50 nm (Fig. 7C). On the ends of some filaments there were knobs (Fig. 7B, open arrows). Transferring the GCG preparation from water into ASW (Fig. 7D) restored the characteristic morphology of microfibrils that had not been equilibrated in deionized water. The morphological changes

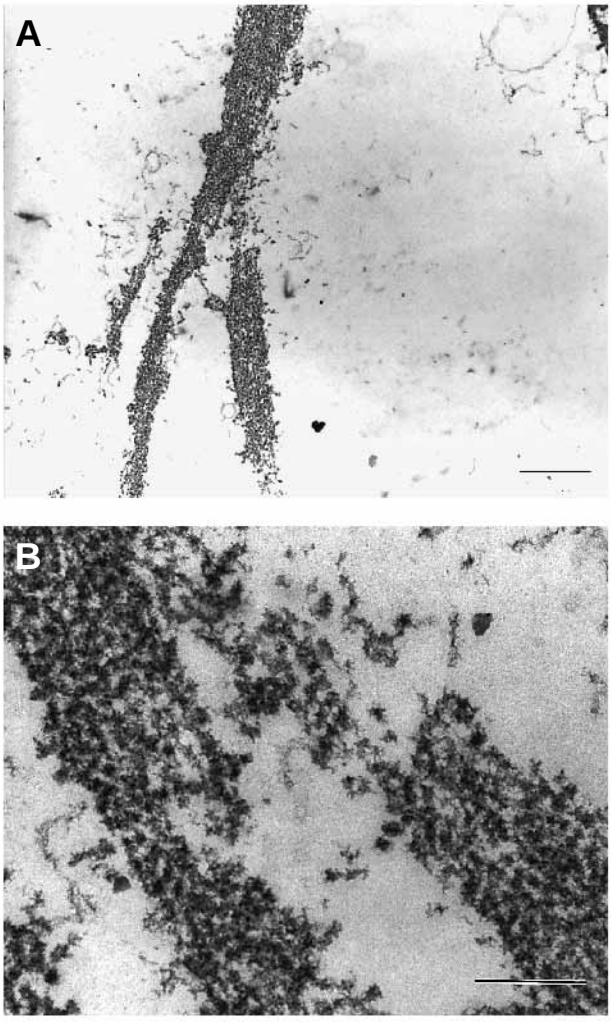

Fig. 4. Transmission electron micrographs of a GCGR (see Materials and methods) microfibrillar preparation. Large clumps of microfibrils can be seen. The morphology is less fibrillar and more stellate than before reduction (compare with Fig. 3). Scale bars, A, 1 μm; B, 300 nm.

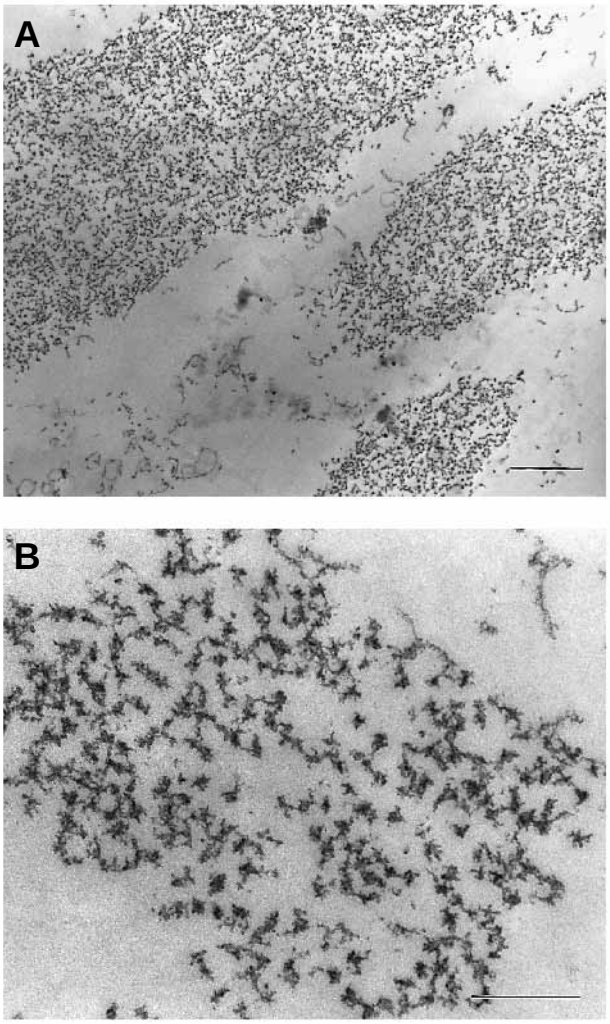

Fig. 5. Transmission electron micrographs of a GCGRA (see Materials and methods) microfibrillar preparation. Distance between microfibrils in bundles is increased over unreduced and reduced specimens (compare with Figs 3 and 4). Scale bars, A, 1 μm; B, 300 nm.

associated with transferring microfibrils from ASW to water were therefore reversible.

Microfibrils transferred from water into 20 mmol l^{-1} $CaCl_2$, 10 mmol l^{-1} Mops, pH 8.0, appeared generally similar to those in ASW, with overlapping filaments (Fig. 7E). Reduced and alkylated microfibrils in ASW or water had approximately the same diameter as unreduced microfibrils, but did not have definable beads and appeared to be made of a tangle of filaments (Fig. 7F).

Tensile testing

Microfibrillar networks (GCG specimens) were tested in tension using a specially fabricated light-duty material testing device. Specimens immersed in temperature-controlled solutions were stretched between two acrylic clamps with known loads. The specimens showed behavior characteristic of a viscoelastic solid (Fig. 8). A 1.6 g load caused a typical specimen to elongate to more than twice its starting length in the first 5 s and to greater than 90 % of the equilibrium length for this load within the first minute. After being loaded for 20 min, the load was removed and the specimen recovered its initial length. It recovered more than 75 % of the elongation within 2 s of being released and more than 95 % of the total elongation within the first 2 min. Of 18 specimens that were each tested for 18 h, none showed detectable creep after the first hour of loading and all returned to their starting length within 2 h after the load had been removed.

GCG, GCGR and GCGRA specimens tested in ASW showed prominent differences in their mechanical behavior. All specimens, regardless of treatment, failed at strains of approximately 2.75 and at loads of 5 g (Fig. 9; Table 3). The load–extension curves for GCG specimens were nearly linear. In striking contrast, the GCGRA specimens had markedly inflected load–extension curves in which less than 20 % of the

breaking load produced more than 80 % of the extension (Fig. 9). GCGR specimens were intermediate between these two extremes. GCG specimens tested in water were even more compliant than GCGRA specimens tested in ASW (Fig. 9) and failed at very low loads.

TEM analysis showed that specimens stretched in ASW contained many microfibril bundles that were aligned with the direction of stretch (Fig. 10, compare with Fig. 3A), but also contained bundles that were not so aligned (Fig. 10, open arrow).

An elastic modulus may be calculated for these specimens, but its significance is not clear since most of the tissue preparation is composed of solvent (Fig. 3A). The elastic modulus of the whole specimen was $7.3\times10^{3}\,N\,m^{-2}$ (Fig. 9) but, because the GCG-treated network in ASW was 96.35 % solvent and 3.65 % microfibrillar mass, the elastic modulus of the microfibrillar component was estimated to be approximately $0.20\times10^{6}\,N\,m^{-2}$.

Each specimen was tested to determine its load–extension relationship and was then loaded until failure. Even though the

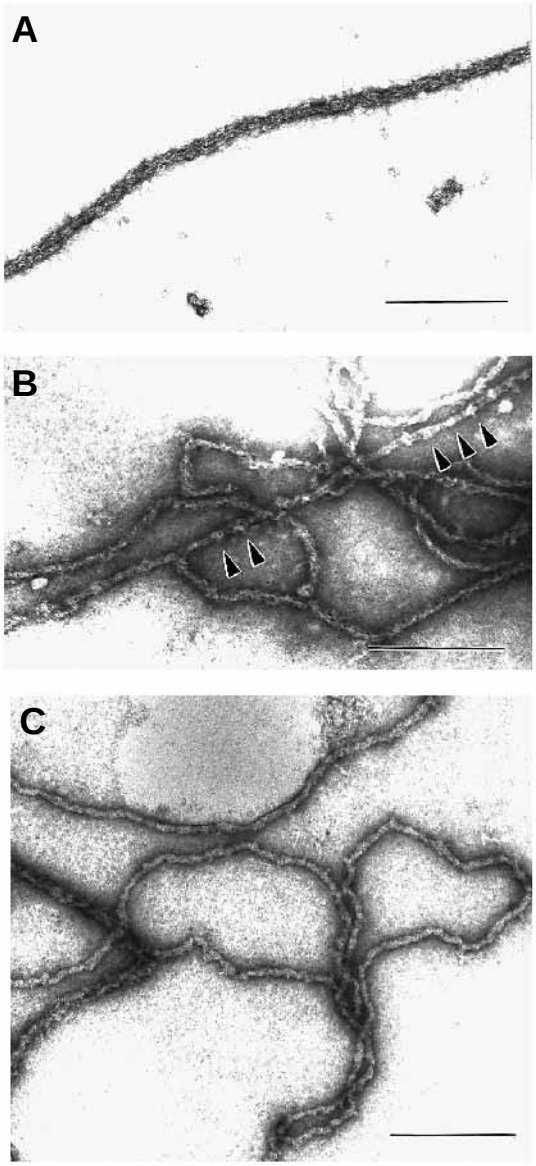

Fig. 6. (A) Transmission electron micrograph of a GCG preparation (see Materials and methods) washed into water and negatively stained with uranyl acetate. The filamentous and helical features of the microfibril in water can be seen. (B) GCG preparation (see Materials and methods) washed into water, Dounce-homogenized and mixed overnight with 20 mmol l^{-1} $CaCl_2$. Beads are present in the structure of some microfibrils (arrowheads). (C) GCGRA specimen (see Materials and methods) washed into water, and negatively stained with uranyl acetate. Scale bars, 200 nm.

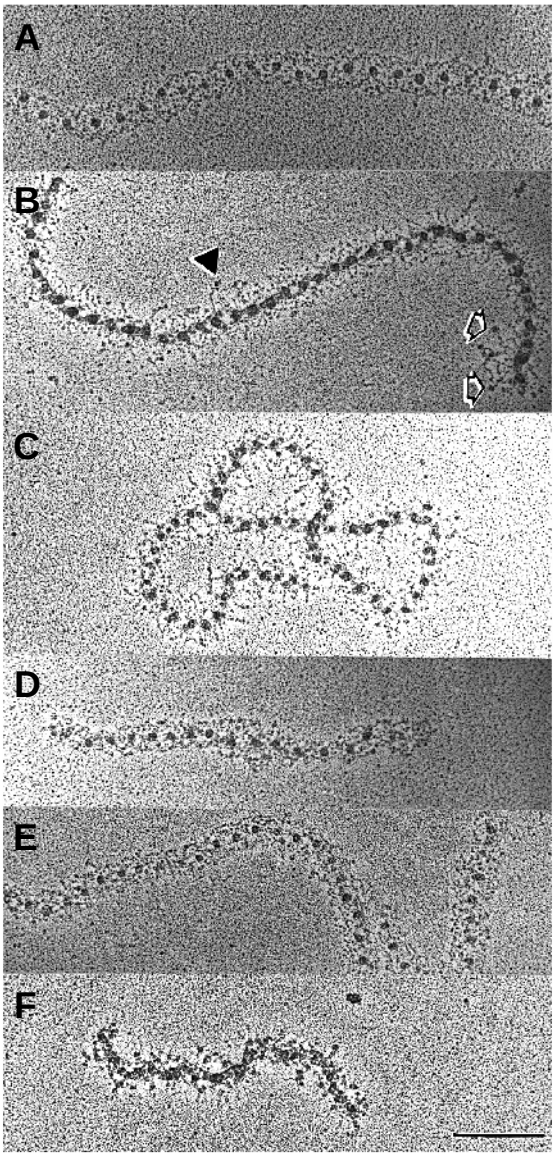

Fig. 7. Transmission electron micrographs of rotary-shadowed microfibril preparations. (A) Microfibril in ASW. (B) GCG specimen (see Materials and methods) swollen in water. Very extended filaments (filled arrowhead) and globular entities on the ends of the filaments (open arrows) can be seen. (C) GCG preparation swollen in water. (D) GCG preparation swollen in water and washed overnight into ASW. (E) GCG preparation swollen in water and washed overnight into 20 mmol l^{-1} $CaCl_2$. (F) GCGRA preparation (see Materials and methods) swollen in water. Scale bars, 200 nm.

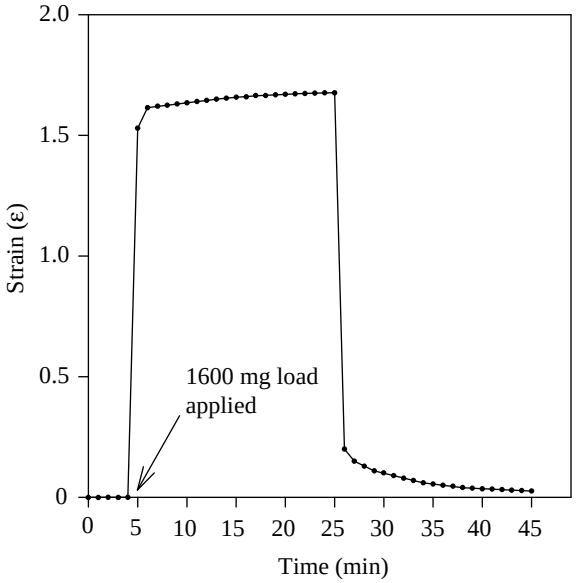

Fig. 8. Diagram of viscoelastic behavior of a GCG-treated (see Materials and methods) microfibrillar network in ASW. At 4 min, the specimen was loaded with 1600 mg. Note that the specimen creeps under a load. At 26 min, the load was removed and the specimen was allowed to recoil. The specimen did not instantaneously return to its initial length. 30–60 min in the unloaded condition was required for the specimen to return to pre-strained length.

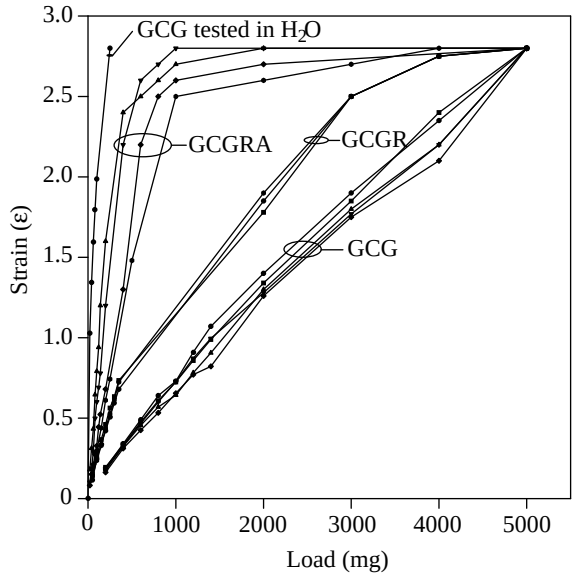

Fig. 9. Load–extension diagram for the microfibrillar specimens, GCG-treated (N=5), GCGR-treated (N=3) and GCGRA-treated (N=4), tested in tension in ASW, and for a typical GCG specimen tested in water. All tests were performed at 12 °C. Specimens ruptured at 275–300 % strain under a load of 4800 mg, except the specimen in water, which ruptured at a much lower load, 300 mg.

elastic stiffness of the specimens decreased after reduction of disulfide bonds and dropped further with reduction and alkylation, the breaking strength of the network remained

Table 3. *Results from tensile tests on treated microfibrillar network preparations*

Specimen	N	Breaking stress (kPa)	Strain at rupture (%)
GCG	9	13 856±4400	275±19.5
GCGR	9	15 735±3965	275±22.5
GCGRA	7	14 047±2476	275±28.7

GCG specimens were sequentially guanidine-extracted, collagenase-digested and guanidine-extracted.

GCGR specimens were treated as GCG followed by reduction with dithiothreitol.

GCGRA specimens were treated as GCG followed by reduction with dithiothreitol and alkylation with iodoacetamide.

Values are means ± S.D.

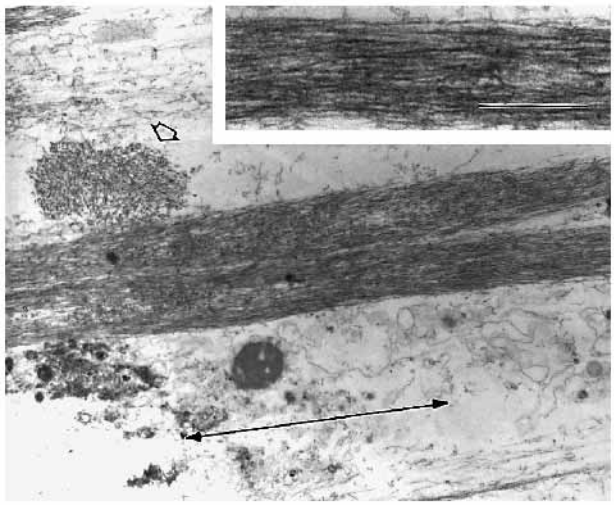

Fig. 10. Transmission electron micrograph of a GCG preparation (see Materials and methods) stretched to 250 % strain, fixed, stained and sectioned. Notice the alignment of the microfibrillar bundles. The double-headed arrow denotes the direction of tissue stretch. The open arrow indicates a microfibril bundle cut in cross section that does not appear stretched. Inset, high magnification of a stretched microfibril bundle. Scale bar, 1 μm; inset, 300 nm.

constant (Table 3). The GCG material was able to store more elastic (strain) energy (proportional to the area between the ordinate and the curve) than the other two groups of specimens (Fig. 9).

Discussion

Microscopy and biomechanical testing have shown that the microfibrillar network of the dermis of the sea cucumber *Cucumaria frondosa* is a continuous, insoluble, non-collagenous network with long-range elastic properties. Exhaustive guanidine extraction and collagenase digestion left a residue that retained the shape of the dermis. This residue was composed principally of microfibrils that were morphologically very similar to the fibrillin microfibrils of mammals. The morphology and material properties of the

network were influenced by the presence or absence of disulfide bonds in the microfibrils and by the ionic composition and pH of the medium with which the network was equilibrated. The lack of solubility and long-range elasticity of the network also indicate that it is probably stabilized by one or more types of non-reducible permanent crosslinks.

Microfibrils of this general morphology have been reported for higher vertebrates (Goldfischer *et al.* 1985; Inoue and LeBlond, 1986), primitive vertebrates (Davison *et al.* 1995) and invertebrates (Grimstone *et al.* 1958; Smith *et al.* 1981; Trotter and Koob, 1989; Candia Carnevali *et al.* 1990; Shadwick *et al.* 1990; Martin and Hose, 1992; Thurmond and Trotter, 1992; Wilkie *et al.* 1992*a*,*b*; Birenheide and Motokawa, 1994; Trotter *et al.* 1994). Rotary-shadowed microfibrils from *C. frondosa* are very similar to fibrillin microfibrils from mammals (Maddox *et al.* 1989; Keene *et al.* 1991; Kielty *et al.* 1991; Ren *et al.* 1991; Sakai *et al.* 1991; Wallace *et al.* 1991; Kielty and Shuttleworth, 1993*a*,*b*; Wright *et al.* 1994), other vertebrates (Wright and Mayne, 1988) and a jellyfish (Reber-Muller *et al.* 1995). The features of shadowed fibrillin microfibrils and of the microfibrils from *C. frondosa* include circular beads about 15 nm in diameter, spaced 45 nm apart, connected to one another by 'arms' or 'filaments'. As shown by Wright and Mayne (1988) and Keene *et al.* (1991), the distance between the beads in mammalian fibrillin microfibrils may be variable, but the beads appear unchanged and connected by filaments. This was also seen in some microfibrillar preparations from *C. frondosa*. Keene *et al.* (1991) measured variations in the interbead distance of fibrillin microfibrils in stretched and unstretched mammalian specimens. They showed that the period commonly varied between 33 and 94 nm, and found specimens with interbead distances as large as 165 nm. This variable interbead spacing may relate to the molecular elastic mechanism, since networks of microfibrils from *C. frondosa* were extensible to about three times their initial length.

Reduction and alkylation markedly changed the appearance and packing of the microfibrils and also greatly reduced the elastic stiffness of the microfibrillar network. Vertebrate fibrillin microfibrils contain multiple epidermal growth factor (EGF) domains with Ca^{2+}-binding properties that depend on disulfide bonds (Handford *et al.* 1991, 1995; Corson *et al.* 1993) and show morphological variations (similar to those reported here) after reduction and alkylation or removal of divalent cations (Kielty and Shuttleworth, 1993*a*). The importance of disulfide bonds in mammalian microfibrils is also shown by the ability of reducing agents to solubilize fibrillin from 'immature' mammalian tissues (Sakai, 1990). The failure of reduction and alkylation to solubilize microfibrils from either adult vertebrate tissues or *C. frondosa* dermis indicates that in both cases the mature microfibrils are stabilized by one or more non-reducible covalent crosslinks. This proposal is strengthened for *C. frondosa* microfibrils by the failure of reduction and alkylation to change the ultimate tensile strength of the microfibrillar network. We will show in a separate publication that the microfibrillar network of *C. frondosa* has a high density of a transglutaminase-derived crosslink, ε-(γ-glutamyl)lysine (F. A. Thurmond, T. J. Koob, J. M. Bowness and J. A. Trotter, in preparation).

Removal of ions from *C. frondosa* microfibrillar networks by extensive equilibration in water led to morphological changes that were similar to those that have been reported for vertebrate microfibrils either not fixed with glutaraldehyde before rotary shadowing (Wright and Mayne, 1988; Ren *et al.* 1991) or treated with EDTA before being shadowed (Kielty and Shuttleworth, 1993*a*).

The material properties of this network clearly demonstrated it to be a long-range elastomer with an important viscous component. The findings that a stable equilibrium length was attained after 1 h and that full recovery was attained after the load had been removed indicate that the amount of plastic deformation in this network is negligibly small.

It is remarkable that the load–extension curve for a GCG specimen was linear throughout its entire range of extension. In comparison, the load–extension curve for elastin is particularly J-shaped, becoming steeper at extensions greater than 100 % (Gosline, 1976). The biological consequence of this linear elasticity is that the force of retraction is linearly dependent on the magnitude of deformation of the network, up to the breaking strain. After reduction and alkylation, the microfibrillar network is less stiff at lower extensions, and the resulting curves are J-shaped. These results indicate that the linear elasticity of the network is dependent on disulfide-bond-dependent structures or interactions.

The protein rubbers (resilin, elastin, abductin, octopus arterial elastomer) are extracellular elastomers whose molecular biomechanics have been extensively described (Shadwick and Gosline, 1983). Protein rubbers have an elastic mechanism that is entropy-driven (Weis-Fogh, 1960; Gosline, 1976). Some of them (resilin, elastin and octopus arterial elastomer) have limits of elasticity in the same range as the sea cucumber fibrillin-like long-range elastomer described in this report (approximately 300 %). Although the data presented here suggest that this material could fall into the class of protein rubbers, tests using the apparatus described have proved difficult to interpret in terms of thermodynamics.

The GCG preparation, as mentioned in the Results section, has an elastic modulus of approximately $0.20\times10^{6}\,N\,m^{-2}$ (when corrected for solvent volume). In mammals, fibrillin microfibrils serve as a scaffolding for the deposition of elastin (Greenlee *et al.* 1966; Cleary *et al.* 1981) and probably have inherent elasticity themselves. It would be expected that the elastic moduli of the fibrillin microfibrillar network and elastin would be compatible. Elastin has an elastic stiffness of $1.2\times10^{6}\,N\,m^{-2}$ (Aaron and Gosline, 1981), which is six times greater than the calculated elastic stiffness of sea cucumber microfibrils ($0.20\times10^{6}\,N\,m^{-2}$). It is important to note that the sea cucumber microfibrillar network is an array of microfibril bundles which interweave with the collagen fibrils and project roughly along the axes of the body of the animal. Even in extended microfibrillar specimens, there were bundles of microfibrils which did not align with the direction of the stretch

and therefore did not participate in the generation of force of retraction. When considering these specimens, only the fraction of the network aligned with the strain direction contributes to the elastic stiffness calculation.

The microfibrillar network displayed the properties of a viscoelastic solid with long-range elasticity. One of two situations must be the case for this network; either (1) it is continuous owing to covalent bonds, or (2) it is sufficiently entangled to give the effect of a continuous network. TEM stereo pairs made from elongated specimens (data not shown) suggested that the individual microfibrils cross over and may branch with one another, as was also seen in rotary-shadowed images of microfibrils. Whether crossovers and branchings represent physical connections between microfibrils or simply entanglements cannot be determined by the methods used here. However, the mechanical consequences are the same for either situation; the network would still possess long-range elasticity, having many effective lateral connections between the elastic microfibrils.

The mechanics of a long-range elastic network from a dermis-like tissue have not been reported for vertebrates, but creep experiments performed by Alexander (1962) on the sea anemone *Metridium senile* strongly suggest the presence of a long-range elastomer in that tissue which allowed reversible extension of the mesoglea by up to three times its initial length. The elastomer in that case was not identified, but the recent observation of fibrillin-like microfibrils in another cnidarian (Reber-Muller *et al.* 1995) suggests that it might be a network of fibrillin-containing microfibrils.

Birenheide and Motokawa (1994) describe 10 nm diameter microfibrils from the aboral ligament of the arm stalk of the deep sea crinoid *Metacrinus rotundus*. They found variable periodicities of the microfibrils between stretched and unstretched specimens within tissue sections. Mechanical tests of the frozen and thawed aboral ligament showed that it was elastic up to at least twice its initial length. The authors suggest that the microfibrils may play an important role as an elastic element in the aboral ligament. The structure of the aboral ligament is generally similar to that of the sea cucumber dermis, with columns of microfibrils running between the bundles of collagen fibrils.

Davison *et al.* (1995) performed inflation tests on aortae from invertebrates and primitive vertebrates which possess no elastin, but have instead an abundance of 10–12 nm diameter microfibrils. They found that the aortae had significant elasticity when inflated and suggested an important role for the microfibrils in the elastic behavior of blood vessels. The microfibrils thus appear to act as an elastomer in several different invertebrate tissues, including blood vessels, dermis and ligaments.

The swelling pressure of a network is equal to the internal osmotic contribution minus the elastic contribution of the network (Comper and Laurent, 1978). For tissues such as articular cartilage, the osmotic pressure is generated by the fixed negative charges of glycosaminoglycans (sulfates and carboxy groups), while positively charged, diffusable counterions, such as Na^+, K^+, Ca^{2+} and Mg^{2+}, offset the negative charges to keep the tissue from swelling significantly. The swelling of the GCG networks in water must be due to a decreased elastic recoil, to an increase in the internal osmotic contribution or to both of these. Sources of the osmotic contribution may include charged residues on the protein or an associated macromolecule, such as an oligosaccharide or a glycosaminoglycan. It will be shown elsewhere that the microfibrillar network contains these three constituents (F. A. Thurmond, T. J. Koob, J. M. Bowness and J. A. Trotter, in preparation). It has been reported that the 10 nm microfibrils in a crinoid are stained by a dye that binds to glycosaminoglycans (Birenheide and Motokawa, 1994), and Chan and Choi (1995) have similarly reported staining of ciliary zonular fibrillin microfibrils with a stain specific for glycosaminoglycans.

The reduction in the volume of the network that was seen when the pH was reduced from 4 to 3 suggests that residues with pK values in this range make a large contribution to the swelling pressure. The pK values of acidic residues on sugars or amino acid side chains in cartilage are as follows (Frank *et al.* 1990): carboxy groups on amino acids, 3.5; carboxy groups on glycosaminoglycans, 3.4; and sulfate groups on glycosaminoglycans, 1.5–2. The shrinkage data therefore suggest that the osmotic contribution was due to the mutual repulsion of negatively charged carboxy groups. Since the volume of the hydrated network also depends on the elastic contribution (recoil) of the network itself, changes in this component cannot be ruled out.

Indeed, reduction and alkylation followed by suspension in water gave the largest degree of swelling for the network. Since it is likely that both intra- and intermolecular disulfide bonds are broken by reduction, the elastic recoil of the network would be minimal and swelling would be maximal when all the disulfide bonds were broken. That disulfide reduction does affect the elastic recoil of the network was shown directly by the load–extension experiments discussed above. Whether the lowered stiffness was due to a direct effect on the protein or to an indirect effect, such as decreased Ca^{2+} binding, is unclear. At any event, the observations that this network has long-range elasticity that depends both on the presence of ions in solution and on disulfide bonds are important new concepts in the biology of the fibrillin family of microfibrils.

Microfibrils play an important role in the organization of elastic tissues throughout the animal kingdom. The current study shows that fibrillin-like microfibrils play a role in the elasticity of sea cucumber dermis. Fibrillin microfibrils may also be an important elastomer in mammals, independent of elastin, as has been suggested by Keene *et al.* (1991) and others. As Reber-Muller *et al.* (1995) point out, the presence of fibrillin-like microfibrils in Cnidaria suggests that this protein family is very old and has been evolutionarily preserved. The data in this report together with previous work suggest that members of the fibrillin family of microfibrils have conferred long-range elasticity to animal connective tissues for at least 550 million years (Davidson *et al.* 1995).

The authors wish to thank Drs Robert Shadwick and Thomas Koob for comments on the manuscript, and Drs Thomas Koob and Gillian Lyons-Levy for helpful discussions and guidance. Also, we would like to thank Dr Iain Wilkie for a copy of a manuscript in press. This work was funded in part by grants from NSF and ONR to J.A.T.

References

AARON, B. B. AND GOSLINE, J. M. (1981). Elastin as a random-network elastomer: a mechanical and optical analysis of single elastic fibers. *Biopolymers* **20**, 1247–1260.

ALEXANDER, R. MCN. (1962). Visco-elastic properties of the body wall of sea anemones. *J. exp. Biol.* **39**, 373–386.

BERGMAN, I. AND LOXLY, R. (1963). Two improved and simplified methods for the spectrophotometric determination of hydroxyproline. *Analyt. Chem.* **35**, 1961–1964.

BIRENHEIDE, R. AND MOTOKAWA, T. (1994). Morphological basis and mechanics of arm movement in the stalked crinoid *Metacrinus rotundus* (Echinodermata, Crinoida). *Mar. Biol.* **121**, 273–283.

CANDIA CARNEVALI, M. D., BONASORO, F., ANDRIETTI, F., MELONE, G. AND WILKIE, I. C. (1990). Functional morphology of the peristomial membrane of regular sea-urchins: Structural organization and mechanical properties in *Paracentrotus lividus*. In *Echinoderm Research* (ed. C. DeRidder, P. Dubois, M.-C. Lahaye and M. Jangoux), pp. 207–216. Rotterdam: Balkema.

CHAN, F. L. AND CHOI, H. L. (1995). Proteoglycans associated with the ciliary zonule of the rat eye: a histochemical and immunocytochemical study. *Histochem. Cell Biol.* **104**, 369–381.

CLEARY, E. G., FANNING, J. C. AND PROSSER, I. (1981). Possible roles of microfibrils in elastogenesis. *Conn. Tissue Res.* **8**, 161–166.

COMPER, W. D. AND LAURENT, T. C. (1978). Physiological function of connective tissue polysaccharides. *Physiol. Rev.* **58**, 255–315.

CORSON, G. M., CHALBERG, S. C., DIETZ, H. C., CHARBONNEAU, N. L. AND SAKAI, L. Y. (1993). Fibrillin binds calcium and is coded by cDNAs that reveal a multidomain structure and alternatively spliced exons at the 5′ end. *Genomics* **15**, 476–484.

DAVIDSON, E. H., PETERSON, K. J. AND CAMERON, R. A. (1995). Origin of bilaterian body plans: evolution of developmental regulatory mechanisms. *Science* **270**, 1319–1325.

DAVISON, I. G., WRIGHT, G. M. AND DEMONT, M. E. (1995). The structure and physical properties of invertebrate and primitive vertebrate arteries. *J. exp. Biol.* **198**, 2185–2196.

ENGEL, J. AND FURTHMAYR, H. (1987). Electron microscopy and other physical methods for the characterization of extracellular matrix components: laminin, fibronectin, collagen IV, collagen VI and proteoglycans. *Meth. Enzymol.* **145**, 3–33.

FRANK, E. H., GRODZINSKY, A. J., PHILLIPS, S. L. AND GRIMSHAW, P. E. (1990). Physicochemical and bioelectrical determinants of cartilage material properties. In *Biomechanics of Diarthroidal Joints*, vol. 2 (ed. V. C. Mow, A. Ratcliffe and S. L.-Y. Woo), pp. 261–282. New York: Springer-Verlag.

GOLDFISCHER, S., COLTOFF-SCHILLER, B. AND GOLDFISCHER, M. (1985). Microfibrils, elastic anchoring components of the extracellular matrix, are associated with fibronectin in the zonule of Zinn and aorta. *Tissue & Cell* **17**, 441–450.

GOSLINE, J. M. (1976). The physical properties of elastic tissue. *Int. Rev. conn. Tissue Res.* **7**, 211–249.

GREENLEE, T. K., JR, ROSS, R. AND HARTMAN, J. L. (1966). The fine structure of elastic fibers. *J. Cell Biol.* **30**, 59–71.

GRIMSTONE, A. V., HORNE, R. N., PANTIN, C. F. A. AND ROBSON, E. A. (1958). The fine structure of the mesenteries of the sea anemone *Metridium senile*. *Q. J. microsc. Sci.* **99**, 523–540.

HANDFORD, P., DOWNING, A. K., RAO, Z., HEWETT, D. R., SYKES, B. C. AND KIELTY, C. M. (1995). The calcium binding properties and molecular organization of epidermal growth factor-like domains in human fibrillin-1. *J. biol. Chem.* **270**, 6751–6756.

HANDFORD, P. A., MAYHEW, M. AND BROWNLEE, G. G. (1991). Calcium binding to fibrillin? *Nature* **353**, 395.

HYMAN, L. H. (1955). *The Invertebrates*, vol. 4 (Echinodermata), pp. 121–138. New York: McGraw-Hill.

INOUE, S. AND LEBLOND, C. P. (1986). The microfibrils of connective tissue. I. Ultrastructure. *Am. J. Anat.* **176**, 121–138.

KEENE, D. R., MADDOX, K. B., KUO, H.-J., SAKAI, L. Y. AND GLANVILLE, R. W. (1991). Extraction of extendable beaded structures and their identification as fibrillin-containing extracellular matrix microfibrils. *J. Histochem. Cytochem.* **39**, 441–449.

KIELTY, C. M., CUMMINGS, C., WHITTAKER, S. P., SHUTTLEWORTH, C. A. AND GRANT, M. E. (1991). Isolation and ultrastructural analysis of microfibrillar structures from foetal bovine elastic tissues. *J. Cell Sci.* **99**, 797–807.

KIELTY, C. M. AND SHUTTLEWORTH, C. A. (1993*a*). The role of calcium in the organization of fibrillin microfibrils. *FEBS Lett.* **336**, 323–326.

KIELTY, C. M. AND SHUTTLEWORTH, C. A. (1993*b*). Synthesis and assembly of fibrillin by fibroblasts and smooth muscle cells. *J. Cell Sci.* **106**, 167–173.

MADDOX, G. K., SAKAI, L. Y., KEENE, D. R. AND GLANVILLE, R. W. (1989). Connective tissue microfibrils: isolation and characterization of three large pepsin-resistant domains of fibrillin. *J. biol. Chem.* **264**, 21381–31385.

MARTIN, G. G. AND HOSE, J. E. (1992). Vascular elements and blood (hemolymph). In *Microscopic Anatomy of Invertebrates*, vol. 10, *Decapod Crustacea* (ed. F. W. Harrison and A. G. Humes), pp. 117–146. New York: Wiley Liss, Inc.

MEANS, G. E. AND FEENEY, R. E. (1975). In *Chemical Modifications of Proteins*, pp. 217–220. San Francisco: Holden-Day.

MOTOKAWA, T. (1984*a*). Viscoelasticity of holothurian body wall. *J. exp. Biol.* **109**, 63–75.

MOTOKAWA, T. (1984*b*). Connective tissue catch in echinoderms. *Biol. Rev.* **59**, 255–270.

MOTOKAWA, T. (1988). Catch connective tissue: a key character for echinoerms' success. In *Echinoderm Biology* (ed. R. D. Burke, P. V. Mladenov, P. Lambert and R. L. Parsley), pp. 39–54. Rotterdam: Balkema.

REBER-MULLER, S., SPISSINGER, T., SCHUCHERT, P., SPRING, J. AND SCHMID, V. (1995). An extracellular matrix protein of jellyfish homologous to mammalian fibrillins forms different fibrils depending on the life stage of the animal. *Devl Biol.* **169**, 662–672.

REN, Z. X., BREWTON, R. G. AND MAYNE, R. (1991). An analysis by rotary shadowing of the structure of the mammalian vitreous humor and zonular apparatus. *J. struct. Biol.* **106**, 57–63.

SAKAI, L. Y. (1990). Disulfide bonds crosslink molecules of fibrillin in the connective tissue space. In *Elastin: Chemical and Biological Aspects* (ed. A. Tamburro and J. Davidson), p. 213. Gelatina: Congedo Editore.

SAKAI, L. Y., KEENE, D. R., GLANVILLE, R. W. AND BACHINGER, H. P. (1991). Purification and partial characterization of fibrillin, a cysteine-rich structural component of connective tissue microfibrils. *J. biol. Chem.* **266**, 14763–14770.

SHADWICK, R. E. AND GOSLINE, J. M. (1983). Molecular biomechanics of protein rubbers in molluscs. In *The Mollusca: Metabolic Biochemistry and Molecular Biomechanics*, vol. 1 (ed. P. W. Hochachka), pp. 399–430. New York, London: Academic Press.

SHADWICK, R. E., POLLOCK, C. M. AND STRICKER, S. A. (1990). Structure and biomechanical properties of crustacean blood vessels. *Physiol. Zool.* **63**, 90–101.

SMITH, D. S., WAINWRIGHT, S. A., BAKER, J. AND CAYER, M. L. (1981). Structural features associated with movement and 'catch' of sea urchin spines. *Tissue & Cell* **13**, 299–320.

THURMOND, F. A. AND TROTTER, J. A. (1992). Microfibrils from sea cucumber body wall. *Am. Zool.* **32**, 44A.

TROTTER, J. A. AND KOOB, T. J. (1989). Collagen and proteoglycan in a sea-urchin ligament with mutable mechanical properties. *Cell Tissue Res.* **258**, 527–539.

TROTTER, J. A. AND KOOB, T. J. (1995). Evidence that calcium-dependent cellular processes are involved in the stiffening response of holothurian dermis and that dermal cells contain and organic stiffening factor. *J. exp. Biol.* **198**, 1951–1961.

TROTTER, J. A., LYONS-LEVY, G., THURMOND, F. A. AND KOOB, T. J. (1995). Covalent composition of collagen fibrils from the dermis of the sea cucumber, *Cucumaria frondosa*, a tissue with mutable mechanical properties. *Comp. Biochem. Physiol.* **112** A, 463–478.

TROTTER, J. A., THURMOND, F. A. AND KOOB, T. J. (1994). Molecular structure and functional morphology of echinoderm collagen fibrils. *Cell Tissue Res.* **275**, 451–458.

WALLACE, R. N., STREETEN, B. W. AND HANNA, R. B. (1991). Rotary shadowing of the elastic system microfibrils in the ocular zonule, vitreous and ligamentum nuchae. *Curr. Eye Res.* **10**, 99–109.

WEIS-FOGH, T. (1960). A rubber-like protein in insect cuticle. *J. exp. Biol.* **37**, 889–907.

WILKIE, I. (1984). Variable tensility in echinoderm collagenous tissues: a review. *Mar. Behav. Physiol.* **11**, 1–34.

WILKIE, I. (1996). Mutable collagenous tissues: extracellular matrix as mechano-effector. In *Echinoderm Studies 5* (ed. M. Jangoux and J. M. Lawrence). Rotterdam: Balkema (in press).

WILKIE, I., CANDIA CARNEVALI, M. D. AND BONASORO, F. (1992*a*). Structure and mechanical behaviour of the compass depressors of *Paracentrotus lividus* (Lamarck) (Echinodermata:Echinoidea). In *Echinoderm Research 1991* (ed. L. Scalera-Liaci and C. Canicatti), pp. 99–105. Rotterdam: Balkema.

WILKIE, I., CANDIA CARNEVALI, M. D. AND BONASORO, F. (1992*b*). The compass depressors of *Paracentrotus lividus* (Echinodermata, Echinoida): Ultrastructural and mechanical aspects of their variable tensility and contractility. *Zoomorphology* **112**, 143–153.

WRIGHT, D. W. AND MAYNE, R. (1988). Vitreous humor of chicken contains two fibrillar systems: an analysis of their structures. *J. Ultrastruct. molec. struct. Res.* **100**, 224–234.

WRIGHT, D. W., MCDANIELS, C. N., SWASDISON, S., ACCAVITTI, M. A., MAYNE, P. M. AND MAYNE, R. (1994). Immunization with undenatured bovine zonular fibrils results in monoclonal antibodies to fibrillin. *Matrix Biol.* **14**, 41–49.